Research Square

Preprints are preliminary reports that have not undergone peer review.
They should not be considered conclusive, used to inform clinical practice,
or referenced by the media as validated information.

Oxygen Diffusion Rapidly Quantifies Water Vapor Permeability and Pore- Networks of Building Materials

Victor Ø. With

von@build.aau.dk

Aalborg University

Kirstine M. Frandsen

Artelia A/S

Asbjørn K. Mikkelsen

Aalborg University

Lotte Louise Pedersen

Aalborg University

Tonje Luckenwald

Aalborg University

Patrick Hundevad

Aalborg University

Hicham Johra

SINTEF Community

Per Moldrup

Aalborg University

Rasmus L. Jensen

Aalborg University

Article

Keywords: Water vapor permeability, oxygen gas diffusivity, dry-cup method, bio-based building materials, pore-network tortuosity, Archie's law

Posted Date: November 23rd, 2026

DOI: https://doi.org/10.21203/rs.3.rs-11599455/v1

License: This work is licensed under a Creative Commons Attribution 4.0 International License.
Read Full License

Additional Declarations: No competing interests reported.

Oxygen Diffusion Rapidly Quantifies Water Vapor Permeability and Pore-Networks of Building Materials

Victor Ø. With[a,*], Kirstine M. Frandsen[b,a], Asbjørn K. Mikkelsen[a], Lotte Louise Pedersen[a], Tonje Luckenwald[a], Patrick Hundevad[a], Hicham Johra[c,a], Per Moldrup[a], Rasmus L. Jensen[a,*]

[a]*Aalborg University, Department of The Built Environment, Thomas Manns Vej 23, Aalborg East, 9220, Denmark*

[b]*Artelia A/S, Mariane Thomsens Gade 1C, Aarhus Centrum, 8000, Denmark*
[c]*SINTEF Community, Department of Architectural Engineering, Børrestuveien 3, Oslo, 0373, Norway*

Contact information:

Victor Ø. With:
Email: von@build.aau.dk

Rasmus L. Jensen
Email: rlje@build.aau.dk

Oxygen Diffusion Rapidly Quantifies Water Vapor Permeability and Pore-Networks of Building Materials

Victor Ø. With[a,*], Kirstine M. Frandsen[b,a], Asbjørn K. Mikkelsen[a], Lotte Louise Pedersen[a], Tonje Luckenwald[a], Patrick Hundevad[a], Hicham Johra[c,a], Per Moldrup[a], Rasmus L. Jensen[a,*]

[a]*Aalborg University, Department of The Built Environment, Thomas Manns Vej 23, Aalborg East, 9220, Denmark*

[b]*Artelia A/S, Mariane Thomsens Gade 1C, Aarhus Centrum, 8000, Denmark*
[c]*SINTEF Community, Department of Architectural Engineering, Børrestuveien 3, Oslo, 0373, Norway*

1 ABSTRACT

The ability of a building material to transmit water vapor is essential for indoor air quality, prevention of fungal growth, and overall livability. Today's slow and tedious methods to quantify material moisture performance is a barrier for designing healthy buildings including new sustainable and/or bio-based materials. In this study, we investigated the theoretical relation between water vapor permeability (WVP) and oxygen gas diffusivity (OGD) in porous media and verify this theoretical relation between OGD and WVP for 12 building materials spanding from dense, low porosity to light, highly-porous materials. Measurement time for OGD was typically 50-100 times quicker than for WVP (e.g., from 240 hours to 3 hours) using a newly-developed, high-precision oxygen diffusion chamber compared to using standard Dry-Cup measurements of WVP on the same material samples. As an additional benefit of the OGD method, pore-network characteristics like tortuosity and the Archie's Law coefficient for pore connectivity can be derived from the measurements. The Archies Law coefficient varied from A = 2 (highly connected pores) for fired brick to A = 250 (almost non-connected pore network) for styrofoam (expanded polystyrene) providing a rapid, highly sensitive measure of pore connectivity for oxygen, radon, and water vapor mobility through building materials.

KEYWORDS

Water vapor permeability, oxygen gas diffusivity, dry-cup method, bio-based building materials, pore-network tortuosity, Archie's law

2 INTRODUCTION

The growing emphasis on sustainability, coupled with more stringent regulations regarding the carbon dioxide equivalent (CO_2e) emissions of buildings, compels engineers and construction professionals to reevaluate their building practices and the materials they select. Here, bio-based building materials could be promising as emerging materials due to their embedded CO_2e [1]. The process of developing and certifying these emerging materials is

both expensive and time-intensive. For instance, assessing the water vapor permeability (WVP), defined as the effective diffusion coefficient of water vapor through a porous medium, can require several weeks to complete [2]. The determination of WVP primarily employs the Cup-method [3], which is extensively utilized [4, 5, 6, 7]. This method is suitable for construction and building materials, utilizing a one-chamber (the cup) system and maintaining a consistent water vapor concentration gradient across the sample being tested. This set-up facilitates Fickian diffusion transport and results in a mass increase of the desiccant or saturated aqueous solution contained within the cup. The Cup-method encompasses two scenarios: Dry-Cup and Wet-Cup, which are distinguished by their respective relative humidity (RH) boundary conditions—Dry-Cup (0/50% RH) and Wet-Cup (50/93% RH). In this research, the Dry-Cup method has been employed to minimize the impact of liquid film flow of water molecules adhering to the inner surface of the porous material, a factor that would otherwise necessitate correction [8].

The gas diffusion coefficient, denoted as D_p , is a recognized parameter in the fields of soil science and soil physics. According to Fick's first law of diffusion, D_p is defined as the proportionality constant that relates the gas flux to the gradient of gas concentration within a porous medium, typically soil or sediment [9]. The D_p, along with its dependence on the air-filled porosity of the soil and the disconnection and tortuosity of the air-filled pore network, influences various factors such as soil aeration, the emission and absorption of greenhouse gases (including CO_2, CH_4, and N_2O) from or into the soil, as well as the movement of volatile organic compounds (in contaminated soil sites) and radon from the soil into indoor air within buildings [10]. Initial measurement set-ups and models for D_p were introduced over 120 years ago [11,12], and currently, one-gas-chamber and two-gas-chamber set-ups are extensively documented for the measurement of D_p in soil and analogous porous media samples [13]. The soil-gas diffusivity, represented as D_p/D_0, where D_0 signifies the oxygen diffusion coefficient in free air, is a commonly utilized property for characterizing a soil's overall capacity to facilitate gas diffusion, as D_p/D_0 remains consistent for various gases at a specific temperature [14]. The value of D_0 for any given gas is influenced by its molecular size and temperature [9].

In the domain of building and construction science, the assessment of material gas diffusion coefficients at specified relative humidity levels has predominantly concentrated on measuring the intrusion and emission of substances such as radon and volatile organic compounds. Historically, the more intricate two-chamber method has been utilized, with its methodology elaborated upon in detail by [9]. This approach has been executed in two primary ways: (i) by measuring two counter-diffusing, largely non-reactive gases, typically involving combinations of xenon (Xe), hydrogen (H_2), nitrogen (N_2), or oxygen (O_2), as evidenced in studies by [15, 16, 17] focusing on concrete, cement, and cement paste; or (ii) by measuring a single target gas, such as radon (Rn), carbon dioxide (CO_2), or O_2, which creates an initially steep concentration gradient between the two chambers, as demonstrated in studies by [18, 19, 20] on radon barrier materials, porous building stones like limestone and sandstone, and compacted asphalt mixtures. The majority of prior research has concentrated on conventional mineral materials, leaving higher-porosity, more permeable biobased materials largely unexamined. Recently, [21] implemented a straightforward, rapid one-chamber oxygen diffusion method based on [9] to assess gas transport and pore characteristics of recycled, compacted concrete aggregates for potential use as sustainable road pavement materials. The current study aims to employ the same methodology as [21], adapted from the soil science field [11], but with an innovative emphasis on swiftly quantifying the water vapor permeability (WVP) of building materials applicable to both mineral and biobased materials across a wide spectrum of air-filled porosity and WVP.

The aim of this research is to compare the Water Vapor Permeability (WVP) determined by the Dry Cup method with the oxygen gas diffusivity (OGD) assessed at 50% relative humidity using a straightforward one-chamber gas diffusion apparatus. The study involves

measurements taken from 12 different building materials that cover a wide range of WVP values, utilizing the same intact samples and dimensions for both measurement techniques. This allows us to assess whether the quickly obtained OGD can serve as a reliable indicator for quantifying the WVP of building materials, while also examining the measurement uncertainty associated with the OGD method.

3 RESULTS

3.1 BASIC MEASUREMENTS

By analyzing the fundamental measurements from consecutive tests utilizing the Dry-Cup method alongside the oxygen gas diffusivity (OGD) method, see Figure 1, it becomes evident that the OGD method operates at a significantly faster pace. A single test within the OGD framework can be completed in approximately three hours for materials exhibiting low OGD, in contrast to the Dry-Cup method, which requires about a week.

In Figure 1a, as water vapor permeates the sample and is absorbed by the desiccant, both the sample and the cup experience an increase in weight. Given that the boundary conditions remain constant, the mass increase is expected to follow a linear trend. Figure 1b illustrates the rise in oxygen concentration within the gas chamber. As the difference in oxygen concentration between the gas chamber and the surrounding air diminishes, the OGD method approaches equilibrium over time. It is noteworthy that both methods yield similar rankings in terms of the material's diffusivity, with Wood Wool (WW) identified as the most diffusive material and Expanded Polystyrene (EPS) as the least.

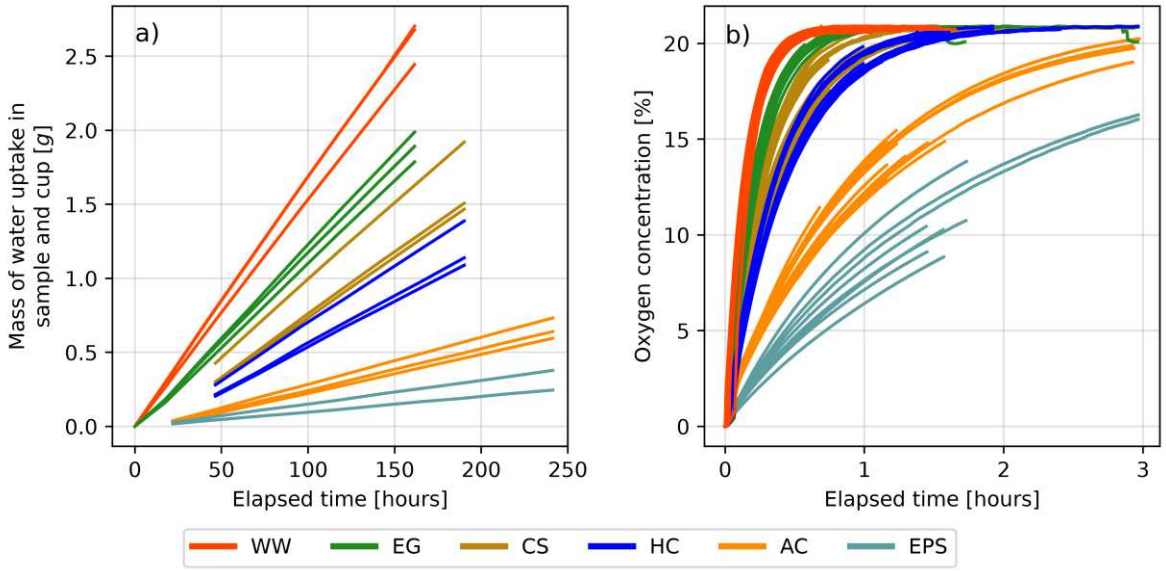

Figure 1 Basic measurements for the two measurement methods, tested as stated in Table 2. a) Dry-Cup method, a steep slope refers to a high water vapor permeability. b) Oxygen gas diffusivity method, a sample with a high diffusivity result in a fast equilibrium with the ambient oxygen concentration (20.9%).

In Figure 1a, the mass change rate (G, kg/s) is ascertained by calculating the slope from the last five days of the data lines, which subsequently allows for the calculation of the WVP in accordance with the methodology outlined in Section 5.1. Figure 1b illustrates the process of obtaining the OGD by converting the curve into a linear form through the application of the

natural logarithm to the measurements, from which the OGD is derived following the procedure detailed in Section 5.2. The results of these measurements are presented in Figure 2.

3.2 THEORETICAL RELATION BETWEEN WATER VAPOR PERMEABILITY AND OXYGEN DIFFUSIVITY

The interrelationship between the water vapor permeability (WVP) and the overall gas diffusion (OGD) can be established by initially characterizing the connection between WVP and water vapor diffusion coefficient (WVGD) as:

$$g = \delta \frac{dp}{dx} \quad and \quad g = D_{H_2O} \frac{dc}{dx} \tag{1}$$

Where g represents the water vapor mass flux (expressed in units of $kg\ (m^2\ s)^{-1}$), which remains constant across both formulations. In the WVP equation (denoted by δ, with units $kg\ (m\ Pa\ s)^{-1}$), the driving force is a pressure differential across the material sample, whereas in the WVGD equation (denoted by D_{H_2O}, with units $m^2 s^{-1}$), the driving force is a concentration gradient. Consequently, these two equations can be equated.

$$\delta \frac{dp}{dx} = D_{H_2O} \frac{dc}{dx} \rightarrow \delta = D_{H_2O} \frac{dc}{dp} \tag{2}$$

The concentration can be ascertained utilizing the ideal gas law, expressed as:

$$c = \frac{m}{V} = \frac{p}{R_{H_2O}\ T} \tag{3}$$

Where m denotes the mass of water vapor contained within an air volume V, p represents the partial pressure of water vapor, R_{H_2O} signifies the specific gas constant for water vapor ($461.5\ J\ (kg\ K)^{-1}$), and T indicates the absolute thermodynamic temperature. By substituting the concentration c in Equation 2 with the expression derived from Equation 3, the following relationship is obtained:

$$\delta = D_{H_2O} \frac{d}{d\left(R_{H_2O}\ T\right)} \tag{4}$$

The conversion of oxygen diffusion to water vapor diffusion has been established since Shimamura [14] demonstrated that the ratio of diffusivity within a sample to diffusivity in free air (D_p/D_0) remains consistent across different gases. Consequently, by determining the diffusivity in free air for both water vapor and oxygen gas, the oxygen gas diffusion (OGD) in a sample can be converted to water vapor gas diffusion (WVGD) as illustrated in Equation 5.

$$\frac{D_{H_2O}}{D_{0,H_2O}} = \frac{D_{O_2}}{D_{0O_2}} \rightarrow D_{H_2O} = \frac{D_{O_2}}{D_{0O_2}} D_{0,H_2O} \tag{5}$$

The diffusivity values in free air (denoted as D_0) are available in scientific literature, with the magnitude of D_0 being temperature-dependent due to molecular kinetic energy. Multiple methodologies have been developed to estimate water vapor diffusivity in free air; Hall et al. [8] evaluated three approaches, yielding WVGD values ranging from $2.47 \cdot 10^{-5}\ m^2\ s^{-1}$ to $2.62 \cdot 10^{-5}\ m^2\ s^{-1}$ at $20°C$. In contrast, Weber et al. [22] employed $2.05 \cdot 10^{-5}\ m^2\ s^{-1}$ for OGD. The combination of Equations 4 and 5 yields the final equation, which expresses the relationship between water vapor pressure (WVP) and OGD.

$$\delta = \frac{D_{O_2}}{D_{0O_2}} D_{0,H_2O} \frac{1}{R_{H_2O}\, T} \quad [6]$$

This gives a linear relationship where D_{O_2}/D_{0O_2} is measured and the slope is $D_{0,H_2O}\ \frac{1}{R_{H_2O}\, T}$. Using the above range of WVGD from [8] yields a slope ranging from $1.81 \cdot 10^{-10}$ to $1.92 \cdot 10^{-10}\ kg\ (m\ Pa\ s)^{-1}$.

3.3 Oxygen diffusivity method compared with Dry-Cup method

Both techniques assess gas diffusion utilizing distinct tracer gases; thus, a notable correlation between these approaches is anticipated when evaluating the results from the analyzed samples. Figure 2 illustrates a robust correlation between the Dry-Cup Method and the OGD Method ($R^2 = 0.99$). All materials were evaluated in accordance with Table 2, and the standard deviation along with the mean value for the OGD measurement was calculated. In the Dry-Cup measurement methodology, the standard deviation and arithmetic mean were calculated for the six designated materials identified in Table 1; conversely, for materials not identified in Table 1, a singular water vapor permeability value was established for each respective material.

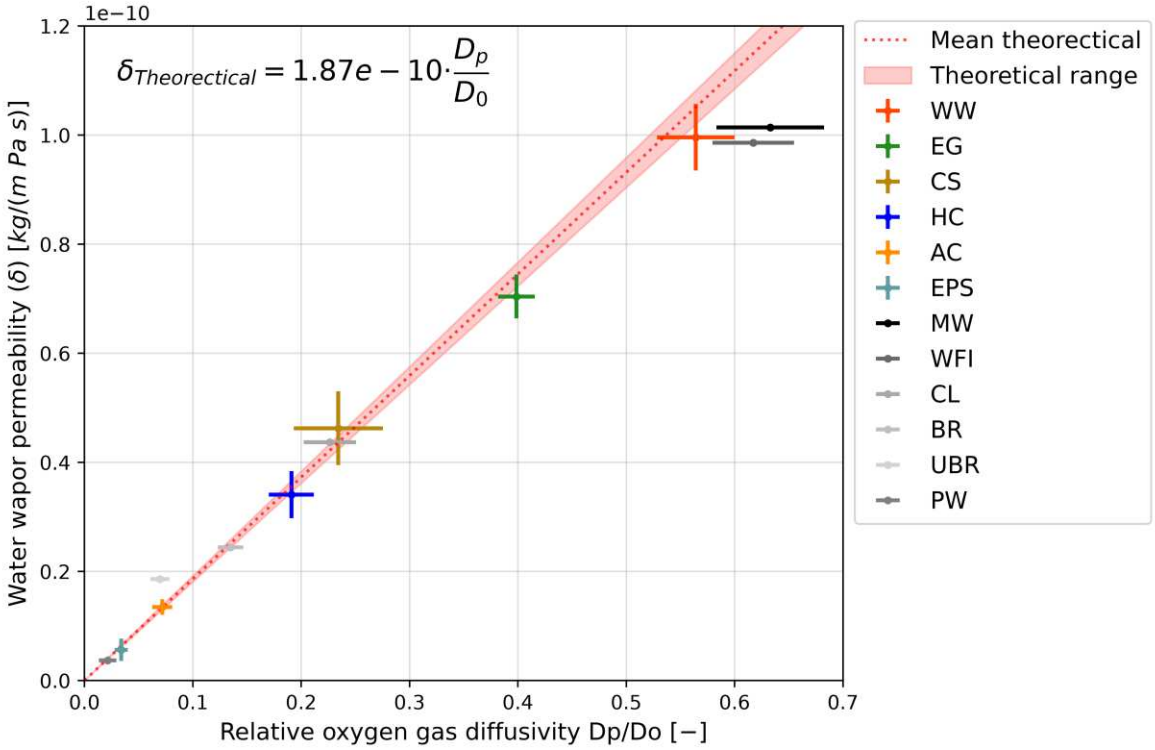

Figure 2 Water vapor permeability and relative oxygen gas diffusivity correlation with horizontal error bars (one standard deviation). For the six selected materials identified in Table 1, tested with multiple cups using the Dry-Cup Method (see Table 2), vertical error bars (one standard deviation) are drawn.

As seen in Figure 2, the fitted trendline diverges from the theoretical line, but most of the measurements reach both the trendline and theoretical line, and the calculated RMSE is close to each other and is smaller than the general uncertainty of the measurement.

3.4 PORE NETWORK TORTUOSITY

The relative oxygen diffusivity can be employed, in addition to estimating the WVP, to ascertain the tortuosity (T) of the sample, which represents the ratio of the diffusion path length through the sample to the sample height. This constitutes a significant material property that facilitates the classification of diverse material types, as it provides insight into the overall pore structure characteristics of a material. T is calculated by:

$$T = \sqrt{\frac{\varepsilon}{\frac{D_p}{D_0}}} \quad [7]$$

In 1942, Archie [23] suggested the following relationship (frequently denoted as Archie's law) to describe the pore network connectivity for various sand and stone samples:

$$\frac{D_p}{D_0} = \varepsilon^A \quad [8]$$

where ε is the air-filled porosity. The combination of the tortuosity factor and Achie's law help to characterize porous materials where a large tortuosity factor indicates a long diffusion path within the material, and a large A indicates a very little connected pore network as seen for EPS in Figure 3b. Figure 3 shows the tortuosity in correlation to the bulk density and air-filled porosity here it is seen that a pure bulk density or air-filled porosity measurement do not by itself tells anything about the pore network. Therefore, the addition of the tortuosity factor and Archie's law helps with understanding the pore network.

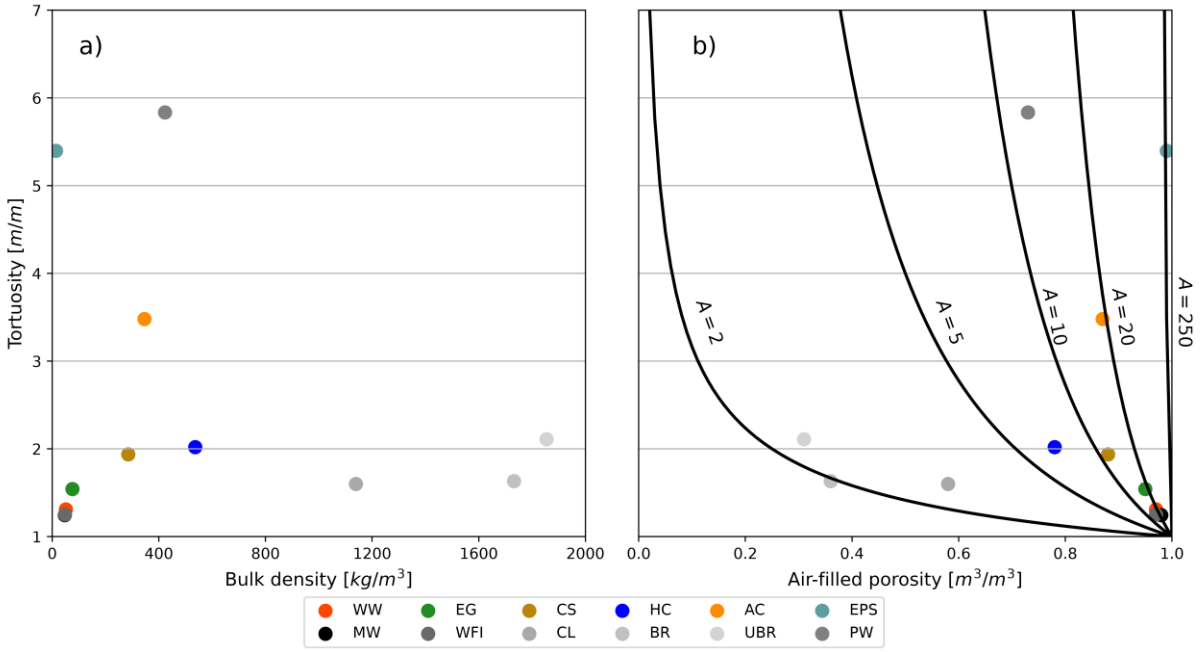

Figure 3 The tortuosities of the 12 materials in relation to their bulk density and air-filled porosity, which serve as useful parameters for categorizing porous materials.

3.5 SCANNING ELECTRON MICROSCOPE IMAGES

The scanning electron microscope (SEM) images provide insights into the pore architecture of each material and reveal the extent of air-filled porosity. For instance, Figure 4b of EPS

displays numerous air pockets with minimal material presence, suggesting a high level of air-filled porosity. Conversely, Figure 4d of UBR tightly compacted clay, which results in a reduced air-filled porosity. Figure 4f illustrates the fibrous pore structure of WW, facilitating gas diffusion, while Figure 4c reveals small fissures in the AC material, which permit only limited gas diffusion indicating a high value for A which is seen in Figure 3b. In Figure 4d it is interesting to see small fibers within the clay mixture, if fibers also were present in the clay mixture of the tested burned brick (BR) then it will leave small air pockets after the burning, therefore the burned bricks should have a higher air-filled porosity and more connected pore-network than the UBR, which is also seen in Figure 3.

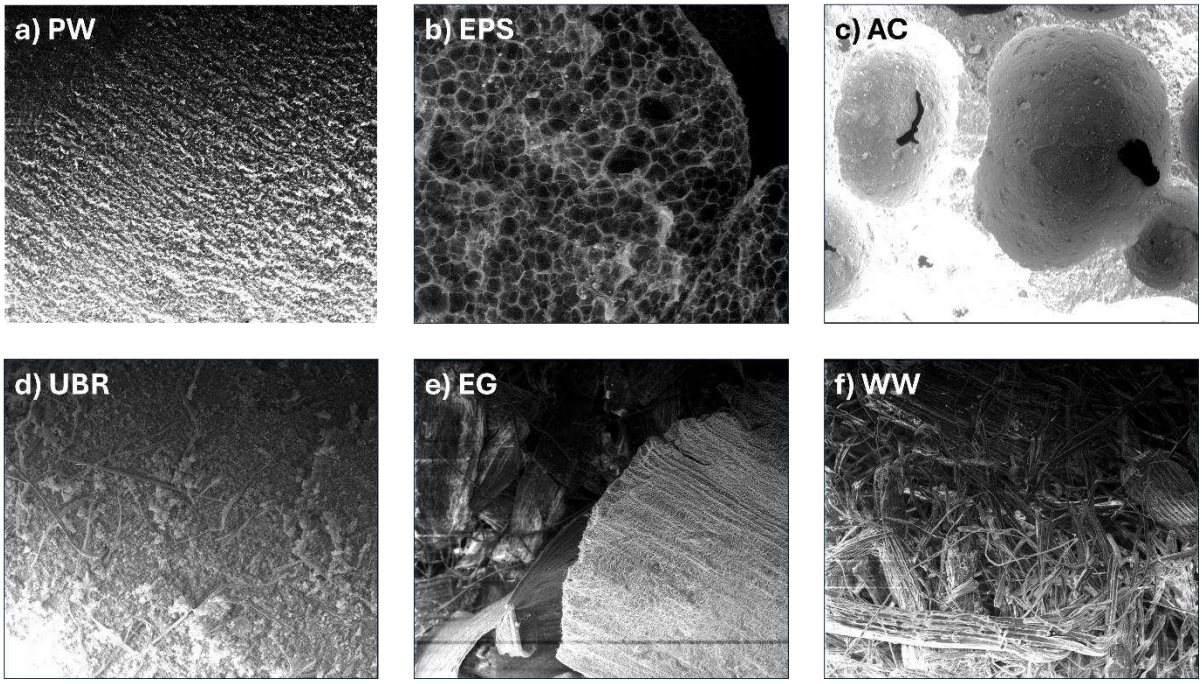

Figure 4 Scanning electron microscope (SEM) photos of selected materials at 100 times magnification. a) Pinewood (PW). b) Expanded polystyrene. c) Aerated concrete (AC). d). Unfired clay brick (UBR). e) Eelgrass insulation (EG). f) Wood wool (WW).

4 DISCUSSION

This paper presents two highly comparable methods both methods utilize a one-chamber system, yet they differ in the tracer gases employed and the boundary conditions of the chamber. The Dry-Cup method incorporates water vapor, a reactive gas that alternates between adhering to porous material surfaces and subsequently releasing, thereby maintaining stable moisture content over time. In contrast, the oxygen gas diffusion (OGD) set-up employs oxygen gas, which is minimally reactive (inert) and diffuses more swiftly through a sample, leading to a reduction in testing duration.

The boundary conditions within the Cup chamber remain constant, while in the OGD chamber, the concentration of oxygen gas increases as it seeks equilibrium with the surrounding air. Consequently, the concentration gradient within the sample is held constant for the Dry-Cup method, whereas it decreases for the OGD method. Given that the

concentration gradients of the samples differ between the Cup and OGD tests, the measurements must be interpreted distinctly. Nevertheless, as illustrated in Figure 2, the error bars for both the Cup and OGD methods exhibit comparable magnitudes of error. This suggests that both methods yield similar performance levels with equivalent uncertainty. For the Dry-Cup method, the boundary humidity conditions range from 0% to 50% RH, while the OGD method maintains nearly constant humidity throughout the sample due to the brief testing duration. Since the difference in magnitude between the computed trendline and the theoretical relationship falls within the same range as the uncertainty, this can be considered negligible. The Dry-Cup method is preferred over the Wet-Cup to facilitate a clear comparison of pure gas diffusivity. In the Wet-Cup, the pore structure is partially saturated with liquid water, which increases the water vapor permeability (WVP) while diminishing the OGD. The influence of these humidity dependencies on OGD necessitates further investigation, where the relative humidity boundary conditions for both the Cup and OGD set-ups should be nearly identical.
This research has presented the implementation of the OGD method for assessing building materials and its potential for rapid measurement of Water Vapor Permeability (WVP). Nonetheless, this method is not fully refined and necessitates additional testing on various materials, as well as further exploration, especially concerning factors such as the enhancement of sample thickness. The OGD apparatus has been constructed, allowing for fast measurements of OGD, whereas the WVP assessments demand a duration that is up to 100 times longer.

As demonstrated in this investigation, oxygen gas diffusion (OGD) measurement constitutes a viable methodology for examining the pore architecture of porous materials. These material characteristics may potentially serve as predictive parameters for estimating the temporally demanding measurement of sorption isotherms across diverse materials, given that tortuosity, Archie's constant, and air-filled porosity can be employed to approximate the internal surface area, which fundamentally influences sorption isotherm behavior.

5 METHODS

5.1 CUP-METHOD FOR MEASURING WATER VAPOR PERMEABILITY

The Cup-method serves as the conventional technique for assessing the Water Vapor Permeability (WVP) coefficient ($kg\ (m\ s\ Pa)^{-1}$) as outlined in EN ISO 12572 [3]. In the Dry-Cup configuration, a desiccant, specifically silica gel, is utilized to maintain an almost 0% relative humidity (RH) within the cup, while the test specimen covers the opening of the cup (refer to Figure 1b). This arrangement establishes a partial pressure gradient of water vapor across the sample, facilitating Fickian diffusion. The permeability is quantified by daily weighing the cup along with the sample and silica gel, which allows for the calculation of the mass flux (the daily change in weight) of water vapor that has diffused through the material and been absorbed by the silica gel. This process results in a consistent linear increase in mass. The test concludes after five consecutive weighings, provided that the mass flux (G) does not vary by more than ±5% from the average G. The WVP is calculated by multiplying G by the thickness of the sample, then dividing by the surface area of the sample and the partial water vapor pressure difference. Additionally, the WVP is adjusted for the air resistance present between the sample and the desiccant (see EN ISO 12572, Appendix G). Prior to the measurements, the samples are conditioned within the same controlled environment, and a sample is deemed conditioned when the five daily weighings show no variation greater than ±5%. Subsequently, the sample is affixed to the cup using a rubber O-ring.
The volume of the cup must be sufficiently large to hold the required quantity of desiccant while also maintaining an air gap between the sample and the desiccant. The requisite amount of

desiccant is defined as the quantity that prevents the air within the cup from reaching saturation during the testing process. As the desiccant takes in water vapor, its efficacy diminishes, leading to a gradual increase in the concentration of water vapor inside the cup over time, which in turn decreases the mass flux. The internal volume of the cup is 342 cm³; however, a portion of this space is occupied by the desiccant, and the volume of the sample is 100 cm³. In this study, six identical cups (C1-C6) were utilized. For one of the cups, Figure 5 illustrates the configuration with a wood wool sample undergoing testing.

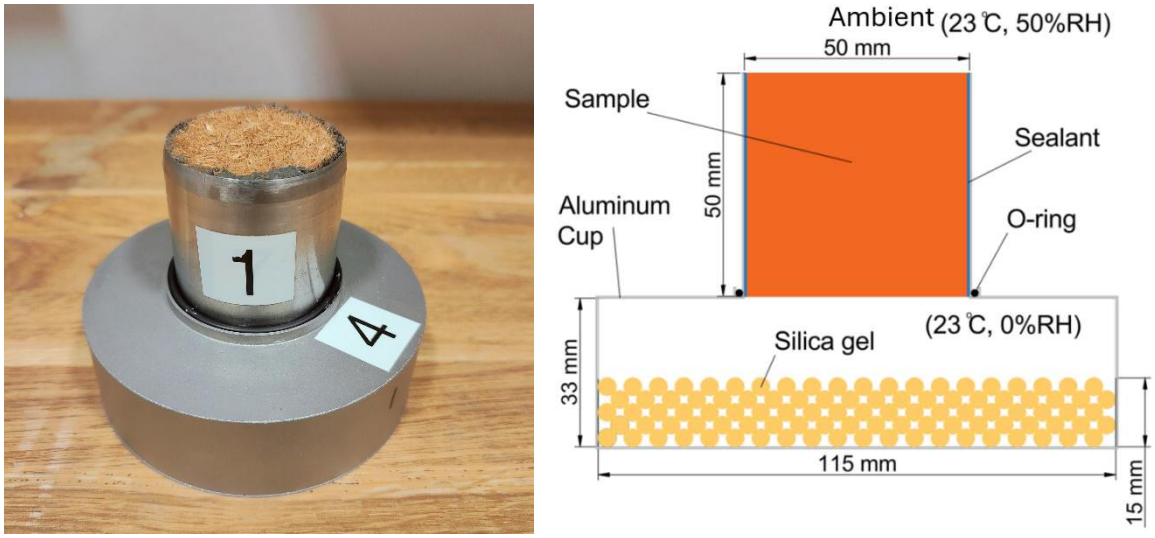

	Temperature	Relative humidity
Initial	$23°C$	$50\%RH$
Ambient	$23°C$	$50\%RH$
Cup	$23°C$	$0\%RH$

Figure 5 Set-up, initial, and boundary conditions used for the Dry-Cup method. a) Assembled cup and sample. b) Set-up dimensions. c) Initial and boundary conditions used for the measurement.

5.2 OXYGEN GAS DIFFUSIVITY

The experimental set-up for measuring the material gas diffusion (D_p, cm^2/s) closely follows guidelines for the one-chamber gas diffusion set-up in [9]. In the present, seven one-chamber set-ups (O1-O7) were constructed in parallel, with each one-chamber set-up fully individually controlled and monitored, thereby allowing for simultaneous measurements on seven intact or repacked material samples.

Briefly, oxygen gas (O_2) was used as the experimental gas. Figure 6 shows the schematic of the one-chamber set-up and the placement of the same wood wool material sample. The chamber is initially flushed with nitrogen (N_2) gas to create an initial near-zero oxygen concentration. At a given time, $t = t_0$, the material sample is then exposed to the ambient atmospheric oxygen concentration at the upper boundary, and the O_2 concentration in the chamber will start increasing due to Fickian diffusion through the material sample, caused by the concentration gradient and controlled by the magnitude of the oxygen gas diffusion (OGD).

To obtain OGD, an analytical solution to Fick's Law of diffusion under the initial and boundary conditions of the experimental set-up was used, together with the measured concentration in the chamber as a function of time. As the O_2 concentration inside the chamber seeks equilibrium with its surroundings, a curve is formed. This curve is transformed into a line, and the slope of the line is determined. The OGD is then computed by multiplying the slope by the porosity and dividing by the first positive root (the root depends on the air-filled porosity and size of the gas chamber) as explained in [9]. To obtain

the relative OGD, D_p/D_0, where D_0 is the oxygen diffusion in free air, a value of $D_0 = 0.205\ cm^2/s$ at $20°C$ was used [22].

In the set-up, a KE-25F3 ($0 - 100\%\ O_2$) sensor [24] sends a 0–10V signal to a datalogger (National Instrument PXIe-4302 [25]). The set-up's combined absolute accuracy is $20mV$. The set-up measures the O_2 concentration as a function of time with a two-second resolution (both ambient concentration at the upper boundary of the sample and concentration in the diffusion chamber). Further details about the one-chamber measurement method and the data analyses to obtain D_p/D_0 are available in [9].

In the Cup-method, the gas-chamber volume is larger than the volume of the sample. The same applies to the OGD set-up, where the gas-chamber's volume is $232cm^3$, approximately 2.3 times greater than the sample volume. In the Cup-method, diffusion is noted by a mass increment, whereas in the OGD method, diffusion is detected as an increase in the oxygen concentration in the gas-chamber.

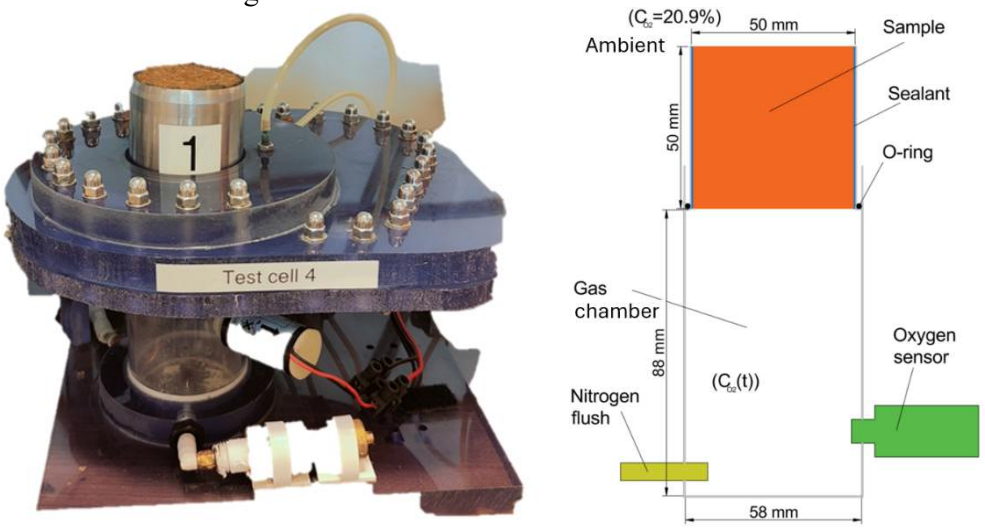

	Temperature	Relative humidity	O_2-concentration
Initial	$23°C$	$50\%RH$	~20.9%
Ambient	$23°C$	$50\%RH$	20.9%
Chamber	$23°C$	$0\%RH$	$0 - 20.9\%$

Figure 6 Set-up, initial, and boundary conditions used for the oxygen gas diffusivity method. a) Assembled gas-chamber and sample. b) Dimensions for the oxygen gas diffusion method. c) Initial and boundary conditions used for the measurement.

5.3 MATERIALS

A total of twelve distinct classical and bio-based building materials were chosen to encompass a broad spectrum of water vapor permeability (WVP) and pore structure characteristics.

Expanded polystyrene insulation (EPS) is frequently utilized in floor construction due to its compressive strength and low WVP. Mineral wool insulation (MW), employed in wall and roof applications, is characterized as a fibrous and highly porous material. Wood fiber insulation (WFI), composed of wood fibers and binders, serves a similar purpose to MW. Wood wool (WW) resembles WFI but is manufactured by a different producer. Eelgrass insulation (EG), derived from stranded eelgrass, contains natural salts. Calcium silicate board (CS) is a high-temperature insulation material known for its properties that prevent fungal growth, attributed to its elevated pH level. Aerated concrete (AC) is a lightweight, precast construction material created from various minerals and cured under pressure and heat in an autoclave. Pinewood (PW) is a widely used construction material. Hempcrete

(HC), a composite of hemp shives and lime binder, is utilized in a manner similar to AC. The clay examined in this study is a raw material suitable for interior wall cladding. Bricks (BR) are conventional construction materials made from clay and subjected to high-temperature firing. Unburned clay bricks (UBR) are formed under high pressure and are intended for internal wall applications. Numerous materials in this study are also analyzed for their water vapor sorption characteristics as referenced in [26].

For all twelve materials, the bulk density in a dry state has been determined using EN 772-3 [27]. For EPS, WW, EG, CS, AC, and HC, the particle density has been assessed using the pycnometer method [28], while the particle density for MW, WFI, PW, Clay, BR, and UBR is derived from lookup values. Table 1 presents a summary of the materials, detailing their bulk and particle density as well as air-filled porosity, which indicates the volume of air contained within a material relative to its overall size.

Table 1: The 12 investigated materials. *Materials selected for method uncertainty analysis.

Material	Bulk density [kg/m^3]	Particle density [kg/m^3]	Air-filled porosity [cm^3/cm^3]	Type
Wood wool insulation (WW)*	50.69	1450	0.97	Commercial - Bio-based
Eelgrass insulation (EG)*	75.69	1390	0.95	Commercial - Bio-based
Calcium silicate (CS)*	285.3	2380	0.88	Commercial - Mineral
Hempcrete (HC)*	536.1	2390	0.78	Non-commercial - Mix
Aerated concrete (AC)*	345.6	2600	0.87	Commercial - Mineral
Expanded polystyrene (EPS)*	13.77	1050	0.99	Commercial - Plastic
Mineral wool insulation (MW)	47.13	2650	0.98	Commercial - Mineral
Wood fiber insulation (WFI)	47.42	1540	0.97	Commercial - Bio-based
Clay (CL)	1139	2700	0.58	Commercial - Mineral
Brick (BR)	1732	2700	0.36	Commercial - Mineral
Unfired clay brick (UBR)	1854	2700	0.31	Commercial - Mineral
Pinewood (PW)	422.5	1540	0.73	Commercial - Bio-based

Out of the 12 materials, six were selected for further analysis, which included various water vapor permeability (WVP) and oxygen gas diffusion (OGD) measurements, as well as scanning electron microscope (SEM) imaging (Zeiss Germany). The selection of these materials was based on their anticipated WVP, ensuring a comprehensive representation across the relevant WVP spectrum. Figure 4 presents the SEM images of the chosen materials, illustrating the significant diversity in their pore structures.

5.4 SAMPLE PREPARATION

Multiple samples of each material have been prepared to assess their WVP and OGD. Each material is shaped into cylinders with a radius of 2.5 cm and a height of 5 cm, which are then secured within a steel ring using sanitary silicone as a sealant. This method guarantees an airtight connection between the steel ring and the material sample, facilitating air diffusion solely through the material rather than at the edges. The assembly of the ring and sample is placed in a chamber where both temperature and relative humidity are regulated (23°C, 50% RH). The identical samples are utilized for the measurements of both WVP and OGD. The number of samples allocated for each measurement is detailed in Table 2

Table 2: Overview of number of samples of each material. The same samples are tested in multiple gas diffusivity set-ups, and each sample is tested in one cup with the Dry-Cup method. For the materials below the two lines, several samples are tested in the same gas diffusivity set-up (set-up 3), where a selected sample of each material is tested in one cup with the Dry-Cup method.

Material	Sample	Gas diffusion set-up							Dry-Cup					
		O1	O2	O3	O4	O5	O6	O7	C1	C2	C3	C4	C6	C6
Wood wool insulation	#1	1	1	1	1	1	1	1	1					
	#2	1	1	1	1	1	1	1		1				
	#3	1	1	1	1	1	1	1			1			
	#4	1	1	1	1	1	1	1						
Eelgrass insulation	#1	1	1	1	1	1	1	1				1		
	#2	1	1	1	1	1	1	1					1	
	#3	1	1	1	1	1	1	1						1
Calcium silicate	#1	1	1	1	1	1	1	1	1					
	#2	1	1	1	1	1	1	1		1				
	#3	1	1	1	1	1	1	1			1			
Hempcrete	#1	1	1	1	1	1	1	1				1		
	#2	1	1	1	1	1	1	1					1	
	#3	1	1	1	1	1	1	1						1
Expanded polystyrene	#1	1	1	1	1				1					
	#2	1	1	1	1					1				
Aerated concrete	#1	1	1	1	1	1	1	1				1		
	#2	1	1	1	1	1	1	1					1	
	#3	1	1	1	1	1	1	1						1
Mineral wool insulation	#1-10			10					#7					
Wood fiber insulation	#1-10			10								#10		
Clay	#1-10			10							#2			
Bricks	#1-10			10									#9	
Unburned clay bricks	#1-10			10						#7				
Pine wood	#1-9			9										#5

5.5 EVALUATION OF MEASUREMENT UNCERTAINTIES

Figure 1b illustrates the fundamental OGD measurements for each sample across the various gas chambers. It is evident that materials exhibiting low OGD levels generally present greater uncertainty compared to those with high OGD, as indicated by the spacing between the curves representing the same type of material. A statistical evaluation of the OGD set-up was conducted to ascertain the extent of the anticipated uncertainty. This uncertainty is calculated by taking the standard deviation and dividing it by the mean value for each sample. Figure 7 depicts the relationship between uncertainty and relative OGD, revealing that materials with elevated OGD levels experience minimal uncertainty (around 3%), while the uncertainty increases significantly for materials with very low permeability.

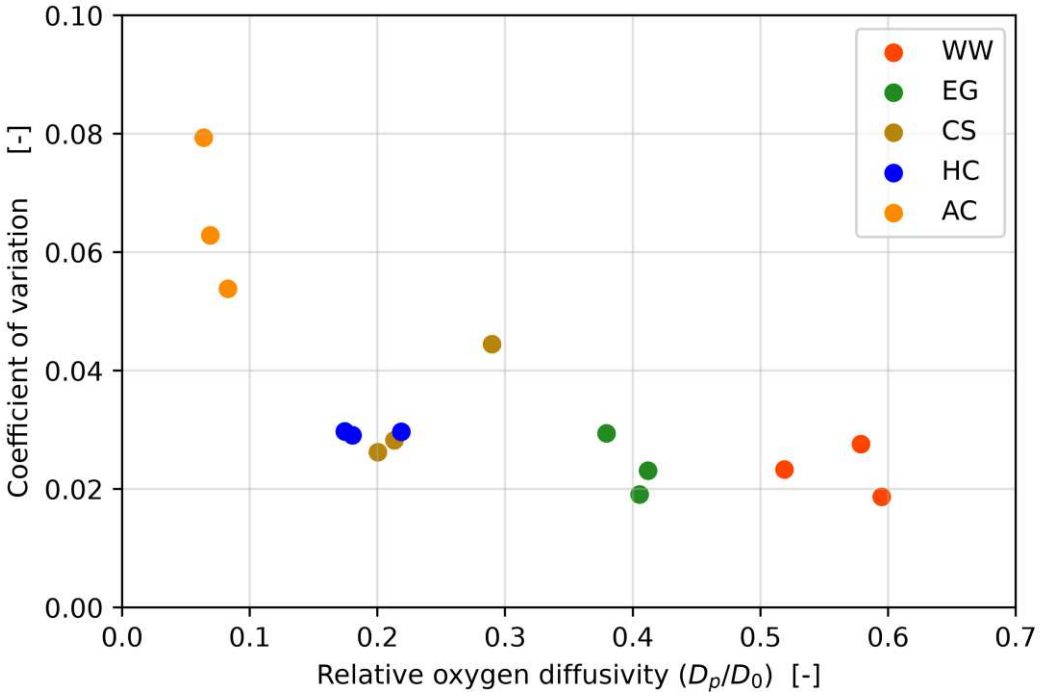

Figure 7 Uncertainty (standard deviation divided by mean) of the oxygen gas diffusivity (OGD) set-up as a function of the relative OGD, each marker represents a sample, and the gray line indicates 3%. The samples are tested according to Table 2.

The error associated with the OGD method does not just stem from an increase in uncertainty for materials with low permeability; it also arises from the failure of the oxygen concentration to achieve equilibrium with the surrounding ambient oxygen levels, as seen in Figure 1b. To mitigate this error, it is advisable to ensure that the oxygen concentration within the gas chamber attains a minimum of 12 − 15%.

6 FUNDING

No funding was received for this study. The research was conducted independently without financial support from any funding agency, commercial organization, or not-for-profit institution.

7 AUTHOR CONTRIBUTIONS

Victor Ørsøe With: Methodology, Investigation, Data gathering, Analysis, Writing. Kirstine Meyer Frandsen: Set-up development, Material gathering. Asbjørn Kaagaard Mikkelsen: Data gathering. Lotte Louise Pedersen: Data gathering. Tonje Luckenwald: Data gathering. Patrick Hundevad: Data gathering. Hicham Johra: Set-up development. Per Moldrup: Methodology, Writing. Rasmus Lund Jensen: Methodology, Writing.

8 DATA AVAILABILITY

Data gathered and analyzed in this study is available in numerical form from the corresponding author by requests.

REFERENCES

[1] Priore, Y. D., Delmenico, S., Rinquet, L., Habert, G. & Jusselme, T. Potential contribution of biogenic materials in new and renovated buildings towards carbon budgets and storage in Switzerland. *J. Clean. Prod.* 147558; https://doi.org/10.1016/j.jclepro.2026.147558 (2026).

[2] Colinart, T. & Glauannec, P. Accuracy of water vapor permeability of building materials reassessed by measuring cup's inner relative humidity. *Build. Environ.* 109038; https://doi.org/10.1016/j.buildenv.2022.109038 (2022).

[3] International Organization for Standardization. *EN ISO 12572:2016 Hygrothermal Performance of Building Materials and Products: Determination of Water Vapour Transmission Properties: Cup Method* (2016).

[4] Perre, P., Casalinho, J., Lancha, J. P. & Remond, R. The extended cup method: Cross-effects of water vapor diffusivity and gas permeability in porous media. *Int. J. Heat Mass Transf.* 126569; https://doi.org/10.1016/j.ijheatmasstransfer.2024.126569 (2025).

[5] Ferrández, D., Zaragoza-Benzal, A., Barrak, E., Santos, P. & Rodrigues, C. Upcycling expanded polyethylene waste for novel composite materials: Physico-mechanical, hygrothermal and life cycle assessment. *Results Eng.* 103535; https://doi.org/10.1016/j.rineng.2024.103535 (2024).

[6] Giuffrida, G., Ibos, L., Boudenne, A. & Allam, H. Exploring the integration of bio-based thermal insulations in compressed earth block walls. *Constr. Build. Mater.* 135412; https://doi.org/10.1016/j.conbuildmat.2024.135412 (2024).

[7] Kabore, A., Laghdir, A. & Ouellet-Plamondon, C. Natural thermal and hygrothermal regulation with heavy cob for low-carbon construction. *Constr. Build. Mater.* 138832; https://doi.org/10.1016/j.conbuildmat.2024.138832 (2024).

[8] Hall, C., Lo, G. J. & Hamilton, A. Water vapour permeability of inorganic construction materials. *Mater. Struct.* **57,** 39; https://doi.org/10.1617/s11527-023-02281-y (2024).

[9] Rolston, D. E. & Moldrup, P. Gas diffusivity in *Methods of Soil Analysis* (Soil Science Society of America, 2002).

[10] Moldrup, P. et al. Structure-dependent water-induced linear reduction model for predicting gas diffusivity and tortuosity in repacked and intact soil. *Vadose Zone J.* https://doi.org/10.2136/vzj2013.01.0026 (2013).

[11] Buckingham, E. *Contributions to Our Knowledge of the Aeration of Soils*. Bulletin No. 25 (USDA Bureau of Soils, Washington, DC, 1904).

[12] Nimmo, J. R. & Landam, E. R. The soil physics contributions of Edgar Buckingham. *Soil Sci. Soc. Am. J.* (2005).

[13] Schjønning, P., Eden, M., Moldrup, P. & de Jonge, L. W. Two-chamber, two-gas and one-chamber, one-gas methods for measuring the soil-gas diffusion coefficient: Validation and inter-calibration. *Soil Sci. Soc. Am. J.* (2013).

[14] Shimamura, K. Gas diffusion through compacted sands. *Soil Sci.* (1992).

[15] Sercombe, J., Vidal, R., Galle, C. & Adenot, F. Experimental study of gas diffusion in cement paste. *Cem. Concr. Res.* (2019).

[16] Zhau, R. et al. Assessment of electrical resistivity and oxygen diffusion coefficient of cementitious materials from microstructure features. *Materials* 3141; https://doi.org/10.3390/ma14123141 (2021).

[17] Lamouchim, T., Levasseur, S., Potier, L., Dubois, T. & Skoczylas, F. About gas permeability and diffusion through concrete. *Mater. Proc.* 42; https://doi.org/10.3390/materproc2023013042 (2023).
[18] Benavente, D. & Pla, D. Effect of pore structure and moisture content on gas diffusion and permeability in porous building stones. *Mater. Struct.* https://doi.org/10.1617/s11527-018-1153-8 (2018).
[19] Wen, Y. & Wang, Y. Determination of oxygen diffusion coefficients of compacted asphalt mixtures. *Constr. Build. Mater.* https://doi.org/10.1016/j.conbuildmat.2017.11.073 (2018).
[20] Tejado-Ramos, J., Alvarez-Toral, A., Guillén, J., Carmona-Carmona, M. & Muñoz-Almaraz, F. J. Methodology for assessment of radon diffusion coefficients in membranes used as radon barriers in construction and refurbishment. *Constr. Build. Mater.* 134967; https://doi.org/10.1016/j.conbuildmat.2024.134967 (2024).
[21] Thai, H. N., Kawamoto, K., Nguyen, H. G., Komatsu, T. & Moldrup, P. Diffusive and convective transport properties and pore-network characteristics of recycled, compacted concrete aggregates for use as road pavement materials. *Constr. Build. Mater.* 139460; https://doi.org/10.1016/j.conbuildmat.2024.139460 (2024).
[22] Weber, P. L., de Jonge, L. W., Greve, M. H., Norgaard, T. & Moldrup, P. Gas diffusion characteristics of agricultural soils from South Greenland. *Soil Sci. Soc. Am. J.* https://doi.org/10.1002/saj2.20114 (2020).
[23] Archie, G. E. The electrical resistivity log as an aid in determining some reservoir characteristics. *Trans. Am. Inst. Min. Metall. Pet. Eng.* **146** (1942).
[24] Figaro Engineering Inc. KE-25F3 oxygen sensor. *Figaro Engineering Inc.* https://www.figaro.co.jp/en/product/.
[25] National Instruments. PXIe-4302. *National Instruments* https://www.ni.com/da-dk/shop/model/pxie-4302.html.
[26] Frandsen, K. M., Antonov, Y. I., Møldrup, P. & Jensen, R. L. Water vapour sorption in twelve mineral and bio-based building materials measured by the Dynamic Dewpoint Isotherm (DDI) method. *Mater. Struct.* **58,** 180; https://doi.org/10.1617/s11527-024-02500-0 (2025).
[27] European Committee for Standardization. *EN 772-3 Methods of Test for Masonry Units: Part 3: Determination of Net Volume and Percentage of Voids of Clay Masonry Units by Hydrostatic Weighing*.
[28] European Committee for Standardization. *EN 1097-7:2022 Tests for Mechanical and Physical Properties of Aggregates: Part 7: Determination of the Particle Density of Filler: Pycnometer Method* (2022).

9 AUTHORS AND AFFILIATIONS

Victor Ø. With[a,*], Kirstine M. Frandsen[b,a], Asbjørn K. Mikkelsen[a], Lotte Louise Pedersen[a], Tonje Luckenwald[a], Patrick Hundevad[a], Hicham Johra[c,a], Per Moldrup[a], Rasmus L. Jensen[a,*]

Victor Ørsøe With
von@build.aau.dk

Rasmus Lund Jensen
rlje@build.aau.dk

[a]*Aalborg University, Department of The Built Environment, Thomas Manns Vej 23, Aalborg East, 9220, Denmark*

[b]*Artelia A/S, Mariane Thomsens Gade 1C, Aarhus Centrum, 8000, Denmark*

[c]*SINTEF Community, Department of Architectural Engineering, Børrestuveien 3, Oslo, 0373, Norway*

10 ADDITIONAL INFORMATION

Competing interests

The author(s) declare no competing interests.

11 LEGENDS

Figure 1. Basic measurements for the two measurement methods, tested as stated in Table 2. a) Dry-Cup method, a steep slope refers to a high water vapor permeability. b) Oxygen gas diffusivity method, a sample with a high diffusivity result in a fast equilibrium with the ambient oxygen concentration (20.9%).

Figure 2. Water vapor permeability and relative oxygen gas diffusivity correlation with horizontal error bars (one standard deviation). For the six selected materials identified in Table 1, tested with multiple cups using the Dry-Cup Method (see Table 2), vertical error bars (one standard deviation) are drawn.

Figure 3. The tortuosities of the 12 materials in relation to their bulk density and air-filled porosity, which serve as useful parameters for categorizing porous materials.

Figure 4. Scanning electron microscope (SEM) photos of selected materials at 100 times magnification. a) Pinewood (PW). b) Expanded polystyrene. c) Aerated concrete (AC). d). Unfired clay brick (UBR). e) Eelgrass insulation (EG). f) Wood wool (WW).

Figure 5. Set-up, initial, and boundary conditions used for the Dry-Cup method. a) Assembled cup and sample. b) Set-up dimensions. c) Initial and boundary conditions used for the measurement.

Figure 6. Set-up, initial, and boundary conditions used for the oxygen gas diffusivity method. a) Assembled gas-chamber and sample. b) Dimensions for the oxygen gas diffusion method. c) Initial and boundary conditions used for the measurement.

Table 1. The 12 investigated materials. *Materials selected for method uncertainty analysis.

Table 2. Overview of number of samples of each material. The same samples are tested in multiple gas diffusivity set-ups, and each sample is tested in one cup with the Dry-Cup method. For the materials below the two lines, several samples are tested in the same gas diffusivity set-up (set-up 3), where a selected sample of each material is tested in one cup with the Dry-Cup method.

Figure 7. Uncertainty (standard deviation divided by mean) of the oxygen gas diffusivity (OGD) set-up as a function of the relative OGD, each marker represents a sample, and the gray line indicates 3%. The samples are tested according to Table 2.